Manipulation of Spin Current in 3*d* Magnets

D. Qu[1] and S. Y. Huang[2]
[1]Institute of Physics, Academia Sinica, Taipei, 11529, Taiwan
[2]Department of Physics, National Taiwan University, Taipei 10617, Taiwan

ABSTRACT

Because of spin-orbit coupling, spintronics has evolved from exploiting spin-polarized current to pure spin current, which delivers spin angular momentum more efficiently with fewer or no charge carriers, enabling spin-orbit torque magnetization switching. In addition to heavy metals, we describe some recent advances, challenges, and prospects for pure spin current in 3*d* magnets, where spin-orbit coupling together with magnetic ordering could open new possibilities for energy-efficient spintronic devices.

INTRODUCTION

Spin-polarized current and pure spin current are vital to spintronics, which utilizes electron spin to store and transfer information. Due to the different electric conductivities between majority and minority spins, electrons flowing in ferromagnetic metals (FM) are spin-polarized. The anomalous Hall effect (AHE) and the anomalous Nernst effect (ANE) in FM are able to generate transverse spin-polarized current by means of the electric field or temperature gradient, respectively [2]. Spin-polarized current transfers its angular momentum through spin-transfer torque (STT), and when it is strong enough, the magnetization is reoriented. On the other hand, due to spin-orbit coupling, a pure spin current with equal numbers of electrons carrying opposite spins may arise both in noble metals and magnets. It has the unique attribute of delivering spin angular momentum with minimal charge carriers [1]. The spin Hall effect (SHE) [3-5], spin pumping (SP) [6], and the longitudinal spin Seebeck effect (LSSE) [7], in conjunction with heavy metals (HMs), FMs, and antiferromagnetic metals (AF) and insulators, generate pure spin currents. The pure spin current enables spin-orbit torque (SOT) [8-10], a mechanism different from spin transfer torque (STT) [11,12], to switch the FM entities, which are essential for high-density memory devices. Previous spin current phenomenon have focused on nonmagnetic metals. This feature article discusses recent advances and prospects for pure spin current in 3*d* magnets.

Transverse spin-polarized current

When a temperature gradient ∇T or an electric field gradient ∇V is applied to a FM metal, a transverse spin-polarized current is generated by the ANE or the AHE, respectively. As shown in Fig. 1(a), the direction of spin-polarized current is perpendicular to both the magnetization and the applied ∇T or ∇V. Notably, both the ANE and AHE in FMs with separation of opposite spins share the same origin of spin-orbit coupling [5]. The spin-dependent voltage induced by the ANE or AHE in various FMs, and caused by the inverse SHE (ISHE) in different nonmagnetic metals, is of either sign. While the sign of the SHE/ISHE is based on the number of valence electrons in s and d orbitals [13], there is no simple rule to determine the sign of the ANE or AHE in FMs.

Fig. 1 (b) shows the ANE for Fe, Co, Ni, and Py, normalized by the distance between the electrical contacts, as a function of the in-plane magnetic field [14]. The spin-polarized current is detected as an electromotive force E by means of the ANE in FMs, which is described by

$$\boldsymbol{E} = \theta_{\mathrm{ANE}} S_{\mathrm{xx}}\, \boldsymbol{m} \times \nabla T. \qquad (1)$$

where $\boldsymbol{m}$ is the unit vector of the magnetic moment, S_{xx} is the longitudinal Seebeck coefficient, and θ_{ANE} is the anomalous Nernst angle, which specifies the charge-to-spin polarized current conversion efficiency. For all FM films, the hysteresis loop of the ANE follows that of the magnetization, as described in Eq. (1). But the sign of the ANE signal is non-trivial. In thicker films, while the sign of the ANE for Fe (50 nm) is opposite to that of Py (30 nm), Co (50 nm), and Ni (50 nm), it is, surprisingly, reversed when its thickness is reduced to 3-nm Fe. Even more interesting is the fact that the magnitude of the ANE signal is enhanced in thinner films of Fe, Co, and Ni, but reduced in Py. The thermal signal induced by the ANE is systematically enhanced with decreasing thicknesses of Co and Fe, but the trend is opposite in Py [14]. Notably, the sign of the ANE for Fe is not always negative, reversing when the thickness is thinner than 6 nm. The magnitude and the sign of S_{xx} are also thickness dependent. The thickness-dependent θ_{ANE}, obtained from Eq. (1), is shown in Fig. 1(c),

The values of θ_{ANE}, for FMs in the bulk region are all around 0.1%–0.2%, which are similar to that of the anomalous Hall angle θ_{AHE}, but the signs of these θ_{ANE} are all positive, unlike θ_{AHE} which can be of either sign. Most importantly, the θ_{ANE} for all four FMs are significantly enhanced by decreasing the thickness. Especially for Fe, Co, and Ni, the θ_{ANE} enhancement is more than ten times for thin films compared with values for bulk samples. The enhancement is attributed to the intrinsic and side-jump mechanisms [14]. The spin-polarized current excited by the ANE is correlated with the Berry curvature around the Fermi level, which could lead to dramatical changes in an ultrathin film. This discovery offers an important guideline for various spin-based thermoelectric applications in spin caloritronics.

Transverse pure spin current

Due to spin-orbit coupling, a charge current $\boldsymbol{j}_C$ in a heavy metal (HM) generates a pure spin current of

$$\boldsymbol{j}_S = (\hbar/2e)\,\theta_{SH}\,\boldsymbol{j}_C \times \boldsymbol{\sigma} \qquad (2)$$

in the transverse direction with the spin index $\boldsymbol{\sigma}$ in the third direction, known as the SHE. The spin Hall angle θ_{SH}, which specifies the charge-to-spin conversion efficiency, can be positive or negative. Many $4d$ and $5d$ HMs have been reported to have large θ_{SH} due to relatively high densities, atomic weights, and atomic numbers [5].

For the LSSE in a HM/FM bilayer, one uses a temperature gradient as shown in Fig. 2 (a), whereas for SP, one uses ferromagnetic resonance (FMR), as shown in Fig. 2(b), to inject a pure spin current into a HM with $\boldsymbol{\sigma}$ set by the magnetization direction of the FM. The resultant pure spin current in the HM is indirectly detected after conversion through the inverse spin Hall effect (ISHE) to a charge current. However, the electrical measurements for spin-to-charge conversion may include unintended charge current effects. The identification and elimination

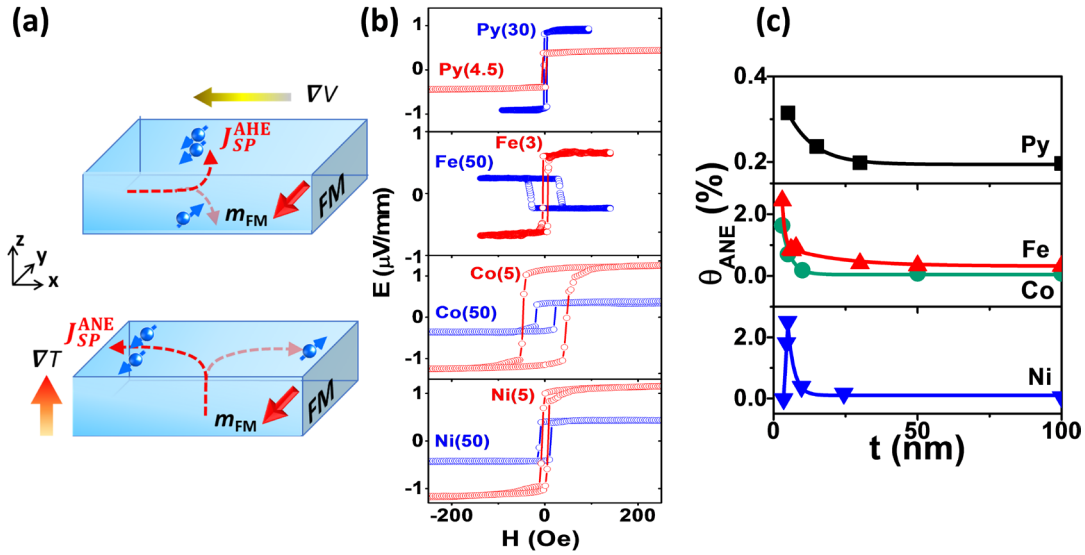

Fig. 1. Schematic illustration of (a) the anomalous Hall effect excited by an electric field (top) and the anomalous Nenst effect excited by a temperature gradient. (b) the anomalous Nernst signal for Fe, Co, Ni and Py as a function of magnetic field. (c) the anomalous Nernst angle as a function of thickness of Fe, Co, Ni, and Py. [14]

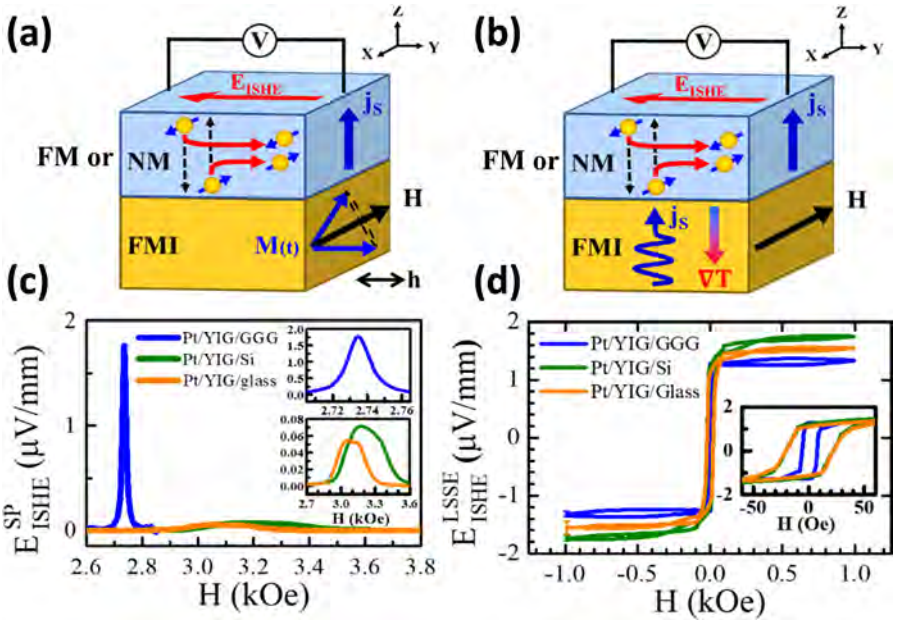

Fig. 2. Schematic illustration of spin current generation form (a) SP and (b) the LSSE. Results of SP measurements (c) and LSSE measuremens (d) on epitaxial YIG thin films on Gadolinium Gallium Garnet (GGG, $Gd_3Ga_5O_{12}$) substrate and polycrystalline YIG films on Si and glass. (a) Normalized FMR absorption intensity. [23]

of the accompanying charge current effects are key challenges in pure spin current phenomena. For example, the use of a FM metal in SP experiments complicates the spin-to-charge extraction because of the various charge effects, including rectification due to the anomalous Hall effect and anisotropic magnetoresistance, the ANE due to FMR heating induced thermal gradients, and other parasitic effects [15-19].

In contrast, the LSSE realized with a ferrimagnetic insulator (FMI), yttrium iron garnet (YIG), has no charge carriers. Using the LSSE, a self-consistent and versatile route to determine the θ_{SH} and spin diffusion lengths λ_{SF} is demonstrated [20]. The SP experiments in HM/YIG, although free from the charge effects in a FM metal such as the ANE, pose other complications. The FMR microwaves, which enable SP, also excite various spin-wave resonance (SWR) modes that complicate the ISHE voltages. [21] The signals from these SWR modes may be separated and extracted in thick (> 50 μm) YIG crystals, but not in thin YIG layers (< a few μm), where the SP and SWR signals are unresolved [22]. Attributing the signals entirely to that of spin-to-charge, as is often done, could exaggerate the SP contribution. It has been found that SWR modes in YIG are more efficient for spin current generation than that of FMR [21, 22].

In addition, the magnitude of spin current generated by SP depends strongly on the quality of the spin injector (e.g., YIG). The SP-induced spin current in polycrystalline YIG films is two-orders-of-magnitude smaller than that in epitaxial YIG films, as shown in Fig. 2 (c) [23]. In contrast, the LSSE excited spin current is surprisingly insensitive to whether the YIG film is epitaxial or polycrystalline, as shown in Fig. 2(d) [23]. In this respect, the robust spin current generated by the LSSE provides superior advantages for exploring spin Hall materials.

Transverse spin current and spin orbit torque in 3d magnet

Through the LSSE, the θ_{SH} and λ_{SF} for various spin Hall materials can be experimentally determined, not only in the heavy 5*d* metals Pt, Ta, W, and Au [20, 24], but also in the 3*d* metals Py [25], Co [26], and Cr [27]. Furthermore, by tuning the atomic percentage, the θ_{SH} in AuTa alloy systems can be tailored [28]. And the enhancement of spin current through spin fluctuation (SF) in spin glass alloy can be achieved [29].

Recently, the enhanced pure spin current due to spin fluctuations in an antiferromagnetic (AF) insulator during the magnetic phase transition has attracted great attention. During the magnetic phase transition, magnetic systems evolve from the long-range ordered magnetic state into the disordered state and exhibit short-range SFs. Thus, it is interesting to explore the short-range ordered spin-glass (SG) system, where the frustrated intra-chain coupling in SG has a significant short-range order associated with large fluctuations.

As shown in Fig. 3 (a), by utilizing the thermally driven spin current of the LSSE in YIG, spin frustrations and spin fluctuations in $Cu_{1-x}Mn_x$ alloys, with various compositions, that result in a transition from the SG state to the AF state, can be investigated [29]. Spin-current enhancement during spin-freezing transition is captured by the temperature-dependent ISHE/SSE measurement for different compositions in $Cu_{1-x}Mn_x$ alloys, as shown in Fig. 3 (b). Initially, the signal increased, reaching a maximum at a peak tempearture T_p and revealing the influence of

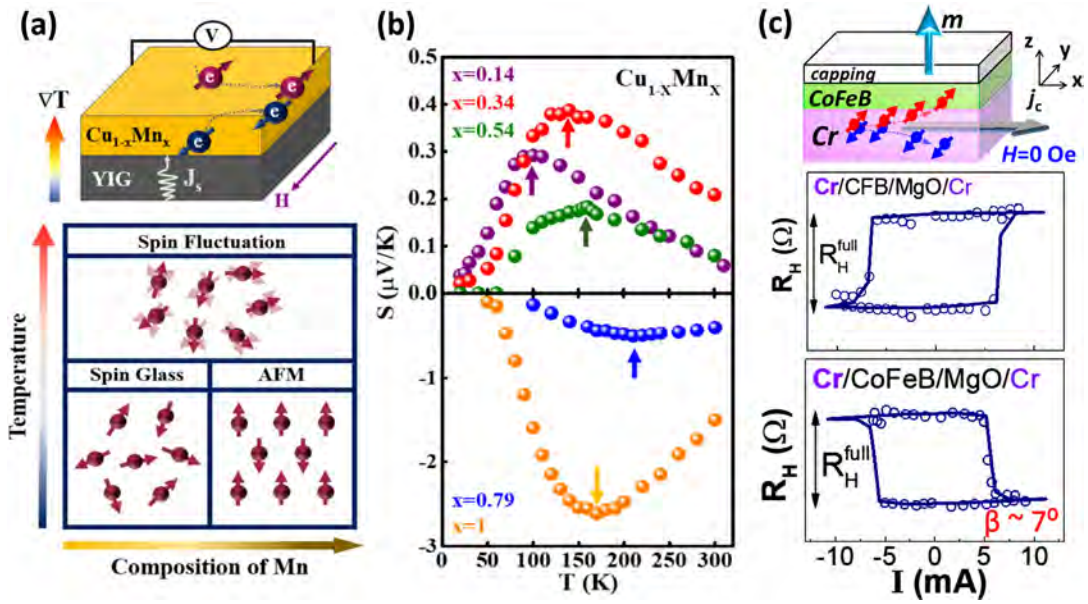

Fig. 3. Schematic illustration of spin current generation due to (a) the magnetic ordering from spin glass to the antiferromagnetic state by increasing the composition of Mn and from the magnetically ordered state to the spin-fluctuation state by increasing temperature. (b) Temperature-dependent spin Seebeck coefficient for $Cu_{1-x}Mn_x$. [29] (c) Schematics of field-free spin-orbit torque (SOT) magnetization switching by applying charge current ($\boldsymbol{j}_C$) in a heterostructure with perpendicular magnetization ($\boldsymbol{m}$) and polarity-controlled field-free SOT switching in Cr/CoFeB/MgO/Cr heterostructures with opposite tilt angle of oblique columnar structures. [39]

SF. The composition-dependent T_p clearly indicates that the SF strongly modulates the magnonic spin current in 3*d* magnetic $Cu_{1-x}Mn_x$ alloys. Notably, the most substantial spin fluctuations occur at T_p, which is considerably higher than the magnetic critical temperature [29]. Consequently, the thermally driven spin current probes the spin susceptibility and the complex spin-freezing process. Furthermore, the results suggest the importance of the effective number of valence electrons in tailoring the spin Hall angle, which specifies the charge-to-spin conversion efficiency, in $Cu_{1-x}Mn_x$ alloys [29].

The discovery of large ISHE in 3*d* magnets by LSSE opens new avenues for spin current explorations, including SOT switching. The transport of spin angular momentum of electrons is exploited to switch magnetic moemnts. The advent of pure spin current enables SOT, a new switching mechanism in three-terminal FM/HM devices, where the switching current passes through the HM layer, peripheral to the vulnerable multilayer stack, thus mitigating the potential damage to the device. The SOT is readily to switch a FM layer with in-plane magnetic anisotropy (IMA) [30, 31], but not a FM with perpendicular magnetic anisotropy (PMA). [32, 33] This is because the spin current generated by the SHE has its spin index $\boldsymbol{\sigma}$ parallel to the interface and perpendicular to the magnetization, and is thus incapable of switching a PMA layer. An additional magnetic field along $\boldsymbol{j}_C$ breaks the up/down symmetry and enables the SOT switching of the PMA layer, but is unsuitable for viable devices. To achieve *field-free* switching of the PMA layer, one may employ various schemes to break the symmetry, including altering the physical shape of the FM layer [34, 35], incorporating an additional magnetic field from exchange bias or another FM layer. [36-38] One scheme is to alter the microstructure of the layer as accomplished in the deterministic field-free switching in Cr/CoFeB/MgO heterostructures with PMA, as shown in Fig. 2 (c).[39] As a result of the off-axis sputtering, a slanted columnar microstructure is created due to the oblique angle deposition and the shadowing effect as shown in Fig. 3(c). The direction of the tilt angle in the columnar microstructure dictates the field-free SOT switching's polarity, as shown in Fig. 3(c). One notes that the Cr layer delivers a comparable switching efficiency to that of the 5*d* Ta-based heterostructure, illustrating that 3*d* materials can exhibit large θ_{SH} [39].

Transverse spin current in 3d antiferromagnet

Previously, since AF (antiferromagnetic) materials with no net magnetization are immune to field interference, the manipulation of AF and AF ordering detection is challenging. Very recently, AF spintronics has become a rapidly developing field. There are theoretical sugges-

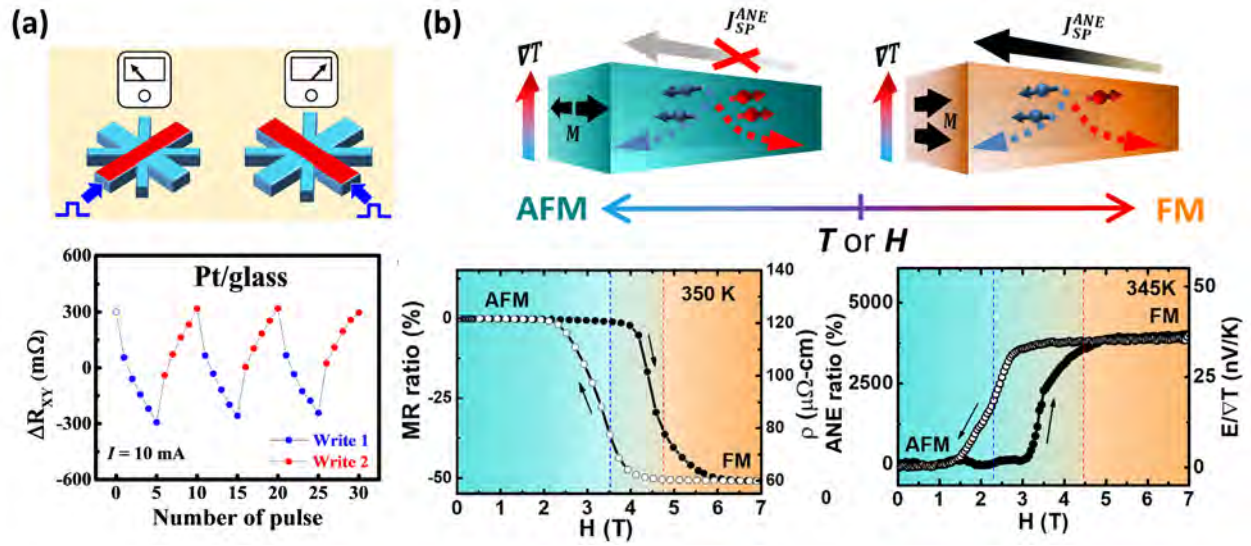

Fig. 4. (a) Schematic illustration of the eight-terminal patterned Pt/glass structure. The relative changes of ΔR_{XY} without the AF layer after applying successive writing pulses current alternately along the 45° and the 135° lines [46]. (b) Schematic illustration of the spin current valve probed by electrical and thermal transport across first-order AFM–FM phase transition in FeRh (top). Field-dependent MR ratio at 350 K and Field-dependent ANE ratio at 345 K (bottom) [50].

tions and experimental claims of electrical switching of the AF Néel vector. The proposal of electrical switching of the AF Néel vector is based on SOT switching, with detection via anisotropic magnetoresistance (AMR) and planar Hall effect (PHE) in conductors or spin Hall magnetoresistance (SMR) in HM-capped insulators. AF switching was first reported in metallic epitaxial thin films of inversion symmetry breaking CuMnAs [40], and later in Mn2Au [41], due to the proposed mechanism of Néel SOT. Later reports claimed AF switching in HM/AF bilayers, such as Pt/NiO [42], Pt/CoO [43], and Pt/Fe_2O_3[44, 45], where HM supplies the spin current for the SOT exerted on the adjacent insulating AF oxide layer.

Most AF switching studies have employed multi- (four or eight) terminal patterned structures, as shown in Figs. 4(a), intended to detect the switching of the AF Néel vector with 90° reorientations. Each current pulse from both orthogonal pairs of leads for the heterostructure of Pt/NiO create the same and reversed incremental resistance change [46]. But this behavior is entirely different from the known SOT and STT switching in FMs. In sharp contrast, there is no change in either STT or SOT switching in FM layersentities after the current density has exceeded the critical value, regardless of the duration of the current or the number of current pulses. Although, these cumulative resistance changes have been attributed to multidomain switching, resulting in incremental resistance increases with a series of current pulses. It is surprising to observe the *same* recurring patterns in resistance change in patterned metallic a Pt layer alone, *without* the AF NiO layer, as shown in Figs. 4(a) [46]. The recurring resistance change could not have been conclusive evidence of SOT switching in AF. This non-magnetic resistance change in Pt comes from anisotropic thermal gradients, non-uniform Joule heating [46], and magnetoelastic stresses [44], the unintended consequences of the multi-terminal patterned structure [47, 48].

AFM switching under a high writing current density of ~10^7A/cm^2, causes intense Joule heating, which leads to irreversible changes in the device due to electromigration and magnetoelastic artifacts. Utilizing AFM as a spin transmission modulator is more promising [49]. FeRh has the unique feature of a phase transition between AFM and FM states around room temperature that modulates the spin current during the first-order magnetic phase transition [50]. As shown in Fig. 4 (b), the electrically and thermally excited spin current probes the first-order phase transition in FeRh. Due to the sharp transition, a large MR ratio of 50% is observed when switching between the AFM and FM states under isothermal conditions, and the ANE induced spin-polarized current's on/off ratio is nearly infinite. The spin-dependent transport behavior in FeRh advances its potential applications for spin current switch devices [50].

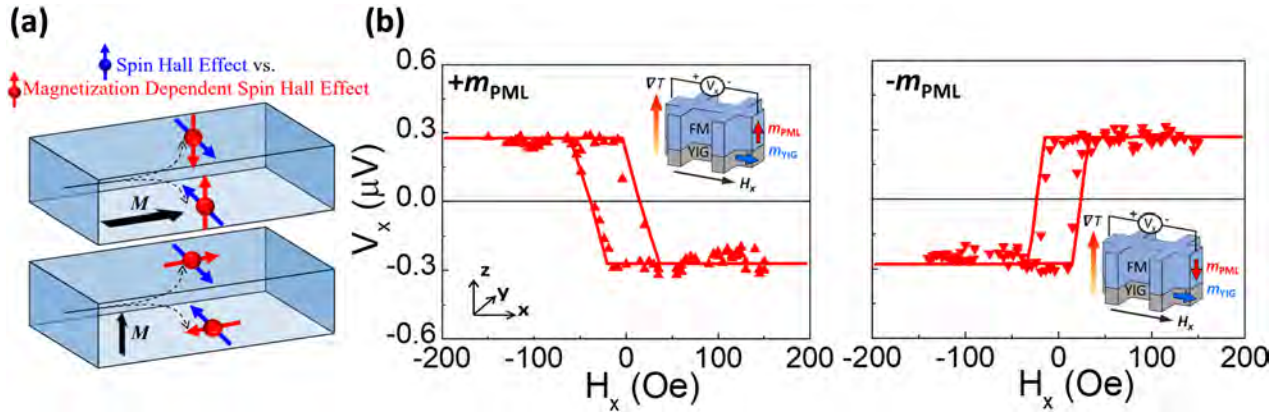

Fig. 5. (a) Schematics of spin Hall and magnetization-dependent inverse spin Hall effect in a ferromagnet (FM). (b) MDISHE voltage for Pt/Co/Pt/YIG with magnetization ($\boldsymbol{m}_{PMA}$) fixed along +z or -z directions. The insets show the experimental setup with magnetic field applied and thermal voltage both measured in the x direction. [56]

Magnetization-Dependent Spin Hall Effect (MDSHE)

In the conventional SHE, the vector cross-product relations among charge current $\boldsymbol{j}_C$, the spin current $\boldsymbol{j}_S$, and spin index $\boldsymbol{\sigma}$ are mutually perpendicular and strictly followed, as shown in Eq. (1). Recent theoretical proposals for interfacial spin-orbit coupling [51], spin swapping [52] and the experimental observations of magnetization-dependent surface spin accumulation [53], spin-orbit torque [38] and the magnetic spin Hall effect [54] suggest that the strict cross-product relation in the conventional SHE may be lifted and generalized to

$$\boldsymbol{j}_S = (\hbar/2e)\,\theta_{MDSH}\,\boldsymbol{j}_C \times (\boldsymbol{\sigma} \times \boldsymbol{m}) \qquad (3)$$

To highlight the magnetization's crucial role, the effect is named the magnetization-dependent spin Hall effect (MDSHE), as illustrated in Fig 5 (a). Experimentally, the unconventional spin accumulation is observed by means of the polar magneto-optic-Kerr-effect measurement [53], the spin Seebeck effect, the second-order planar Hall effect and spin-torque FMR spectroscopy [55] in the all-metallic based heterostructures. However, as noted above, the simultaneous occurrence of the anomalous Hall effect (AHE), PHE, and ANE in the FM metals are unavoidable, and the separation of these parasitic effects is non-trivial.

A better design without the complications in all-metallic structures involves LSSE measurement in the magnetic insulator YIG with PMA (Pt/Co/Pt) situated on top, as shown in Fig. (5) [56]. Under an out-of-plane temperature gradient (*z*-direction), with magnetization of the YIG in the *y*-direction, one measures the ISHE voltage in PMA in the *x*-direction, without the contamination of the AHE or the ANE. Crucially, when the magnetization of the YIG is aligned in the *x*-direction, there is no ISHE in the *x*-direction, but only the MDISHE. In this manner, ISHE and MDISHE are revealed separately and cleanly in the same structure under the same temperature gradient. The ratio of spin Hall angle $\theta_{MDSH}/\theta_{SH}$ is found to be about 3.6%. Thus, the spin orientation in the FM layer is arbitrarily set by the combination of charge current direction and magnetization orientation, which breaks the strict cross-product relation in the conventional SHE [56].

SUMMARY

In this article, the generation, detection, and manipulation of pure spin current in 3*d* magnets have been discussed. Specifically, we discussed the following aspects. The spin-polarized current excited by the ANE is enhanced in FM thin films due to spin-orbit coupling. The spin current robustly excited by the LSSE in YIG is a powerful tool to explore the SHE and spin susceptibility in 3d magnets. The charge-to-spin conversion efficiency θ_{SH} is tuned and enhanced through spin fluctuation in AF insulators and spin glasses. The polarity-controlled field-free SOT switching is due to oblique columnar structures, which is attractive for high-density memory devices. The prospects for electrical switching in AF materials remain controversial, while the virtually infinite spin current on/off ratio is achieved in FeRh during the first-order magnetic phase transition between AF and FM states. Finally, the strict cross product rule of the SHE in all pure spin current phenomena is lift by the newly predicted and clearly observed MDSHE.

Acknowledgements: In collaboration with T. Chuang, C. Chiang, and P. Wu at National Taiwan University and C. L. Chien at Johns Hopkins University. Work at NTU was supported by the Ministry of Science and Technology of Taiwan under Grants No. MOST 106-2628-M-002-015-MY3 and No. MOST 109- 2123-M-002-002. Work at Academia Sinica was supported by the AS Thematic Project No. AS-TP-107-M04 and iMATE Project No. AS-iMATE-109-11.

References

[1] A. Davidsona, V. P. Aminbc, W. S. Aljuaida, P. M. Haney, X. Fan, "Perspectives of electrically generated spin currents in ferromagnetic materials," Physics Letters A, 384, 126228 (2020).
[2] Y. Pu, D. Chiba, F. Matsukura, H. Ohno, and J. Shi, "Mott Relation for Anomalous Hall and Nernst Effects in $Ga_{1-x}Mn_xAs$ Ferromagnetic Semiconductors" Phys. Rev. Lett. 101, 117208 (2008).
[3] M. I. Dyakonov, and V. I. Perel, "Current-induced spin orientation of electrons in semiconductors," Phys. Lett. A 35, 459 (1971).
[4] J. E. Hirsch, "Spin Hall Effect," Phys. Rev. Lett. 83, 1834 (1999).
[5] J. Sinova, S. O. Valenzuela, J. Wunderlich, C. H. Back, and T. Jungwirth, "Spin Hall effects," Rev. Mod. Phys. 87, 1213 (2015).
[6] Y. Tserkovnyak, A. Brataas, G. E. W. Bauer, "Enhanced Gilbert Damping in Thin Ferromagnetic Films," Phys. Rev. Lett. 88, 117601 (2002).
[7] K. Uchida, H. Adachi, T. Ota, H. Nakayama, S. Maekawa, and E. Saitoh, "Observation of longitudinal spin-Seebeck effect in magnetic insulators," Appl. Phys. Lett. 97, 172505 (2010).
[8] K. Ando, S. Takahashi, K. Harii, K. Sasage, J. Ieda, S. Maekawa, and E. Saitoh, "Electric Manipulation of Spin Relaxation Using the Spin Hall Effect," Phys. Rev. Lett. 101, 036601 (2008).
[9] L. Liu, C. F. Pai, Y. Li, H. W. Tseng, D. C. Ralph, and R. A. Buhrman, "Spin-Torque Switching with the Giant Spin Hall Effect of Tantalum," Science 336, 555 (2012).
[10] A. Manchon, J. Železný, I. M. Miron, T. Jungwirth, J. Sinova, A. Thiaville, K. Garello, and P. Gambardella, "Current-induced spin-orbit torques in ferromagnetic and antiferromagnetic systems," Rev. Mod. Phys. 91, 035004 (2019).
[11] J. C. Slonczewski, "Current-driven excitation of magnetic multilayers," J. Magn. Magn. Mater. 159, L1 (1996).
[12] L. Berger, "Emission of spin waves by a magnetic multilayer traversed by a current," Phys. Rev. B 54, 9353 (1996).
[13] T. Tanaka, H. Kontani, M. Naito, T. Naito, D. S. Hirashima, K. Yamada, and J. Inoue, "Intrinsic spin Hall effect and orbital Hall effect in 4d and 5d transition metals," Phys. Rev. B 77, 165117 (2008).
[14] T. C. Chuang, P. L. Su, P. H. Wu, and S. Y. Huang, "Enhancement of the anomalous Nernst effect in ferromagnetic thin films," Phys. Rev. B 96, 174406 (2017).
[15] W. G. Egan and H. J. Juretschke, "DC detection of ferromagnetic resonance in thin nickel films," J. Appl. Phys. 34, 1477 (1963).
[16] M. Harder, Y. S. Gui, and C. M. Hu, "Electrical detection of magnetization dynamics via spin rectification effects," Phys. Rep. 661, 1 (2016).
[17] R. Iguchi and E. Saitoh, "Measurement of Spin Pumping Voltage Separated from Extrinsic Microwave Effects," J. Phys. Soc. Jpn. 86, 011003 (2017).
[18] S. Y. Huang, X. Fan, D. Qu, Y. P. Chen, W. G. Wang, J. Wu, T. Y. Chen, J. Q. Xiao and C. L. Chien, "Transport magnetic proximity effects in platinum," Phys. Rev. Lett. 109, 107204 (2012).
[19] S. Y. Huang, W. G. Wang, S. F. Lee, J. Kwo, and C. L. Chien, "Intrinsic Spin-Dependent Thermal Transport," Phys. Rev. Lett. 107, 216604 (2011)
[20] D. Qu, S. Y. Huang, B. F. Miao, S. X. Huang, and C. L. Chien, "Self-consistent determination of spin Hall angles in selected 5d metals by thermal spin injection," Phys. Rev. B 89, 140407(R) (2014).
[21] C. W. Sandweg, Y. Kajiwara, K. Ando, E. Saitoh, and B. Hillebrands, "Enhancement of the spin pumping efficiency by spin wave mode selection," Appl. Phys. Lett. 97, 252504 (2010).
[22] Y. S. Chen, J. G. Lin, S. Y. Huang, and C. L. Chien, "Incoherent spin pumping from YIG single crystals," Phys. Rev. B 99, 220402(R) (2019).
[23] F.-J. Chang, J. G. Lin, and S.-Y. Huang, "Robust spin current generated by the spin Seebeck effect," Phys. Rev. Mater. 1, 031401(R) (2017).
[24] D. Qu, S. Y. Huang, J. Hu, R. Wu, and C. L. Chien, "Intrinsic Spin Seebeck Effect in Au/YIG," Phys. Rev. Lett. 110, 067206 (2013).
[25] B. F. Miao, S. Y. Huang, D. Qu, and C. L. Chien, "Inverse Spin Hall Effect in a Ferromagnetic Metal," Phys. Rev. Lett. 111, 066602 (2013).
[26] D. Tian, Y. Li, D. Qu, S. Y. Huang, X. Jin, and C. L. Chien, "Manipulation of pure spin current in ferromagnetic metals independent of magnetization," Phys. Rev. B. 94, 020403(R) (2016).
[27] D. Qu, S. Y. Huang, and C. L. Chien, "Inverse spin Hall effect in Cr: Independence of antiferromagnetic ordering," Phys. Rev. B. 92, 020418 (R) (2015).
[28] D. Qu, S. Y. Huang, G. Y. Guo, and C. L. Chien, "Inverse spin Hall effect in Au_xTa_{1-x} alloy films," Phys. Rev. B 97, 024402 (2018)
[29] P.-H. Wu, Y.-C. Tu, D. Qu, H.-L. Liang, S.-F. Lee, and S.-Y. Huang, "Probing the spin-glass freezing transition in $Cu_{1-x}Mn_x$ alloy by spin current," Phys. Rev. B 101, 104413 (2020).
[30] L. Liu, C. F. Pai, Y. Li, H. W. Tseng, D. C. Ralph, and R. A. Buhrman, "Spin-torque switching with the giant spin Hall effect of tantalum" Science 336, 555 (2012).
[31] G. Mihajlovic, O. Mosendz, L. Wan, N. Smith, Y. Choi, Y. Wang, and J. A. Katine, "Pt thickness dependence of spin Hall effect switching of in-plane magnetized CoFeB free layers studied by differential planar Hall effect," Appl. Phys. Lett. 109, 192404 (2016).
[32] I. M. Miron, K. Garello, G. Gaudin, P. J. Zermatten, M. V. Costache, S. Auffret, S. Bandiera, B. Rodmacq, A. Schuhl, and P. Gambardella, "Perpendicular switching of a single ferromagnetic layer induced by in-plane current injection," Nature 476, 189 (2011).
[33] S. Fukami, T. Anekawa, C. Zhang, and H. Ohno, "A spin-orbit torque switching scheme with collinear magnetic easy axis and current configuration," Nat. Nanotechnol. 11, 621 (2016).
[34] G. Yu, P. Upadhyaya, Y. Fan, J. G. Alzate, W. Jiang, K. L. Wong, S. Takei, S. A. Bender, L. T. Chang, Y. Jiang, M. Lang, J. Tang, Y. Wang, Y. Tserkovnyak, P. K. Amiri, and K. L. Wang, "Switching of perpendicular magnetization by spin–orbit torques in the absence of external magnetic fields," Nat. Nanotechnol. 9, 548 (2014).
[35] L. You, O. Lee, D. Bhowmik, D. Labanowski, J. Hong, J. Bokor, and S. Salahuddin, "Switching of perpendicularly polarized nanomagnets with spin orbit torque without an external magnetic field by engineering a tilted anisotropy," Proc. Natl. Acad. Sci. U.S.A. 112, 10310 (2015).
[36] S. Fukami, C. Zhang, S. DuttaGupta, A. Kurenkov, and H. Ohno, "Magnetization switching by spin-orbit torque in an antiferromagnet-ferromagnet bilayer system," Nat. Mater. 15, 535 (2016).
[37] A. van den Brink, G. Vermijs, A. Solignac, J. Koo, J. T. Kohlhepp, H. J. Swagten, and B. Koopmans, "Field-free magnetization reversal by spin-Hall effect and exchange bias," Nat. Commun. 7, 10854 (2016).

[38] S. C. Baek, V. P. Amin, Y. W. Oh, G. Go, S. J. Lee, G. H. Lee, K. J. Kim, M. D. Stiles, B. G. Park, and K. J. Lee, "Spin currents and spin-orbit torques in ferromagnetic trilayers," Nat. Mater. 17, 509 (2018).
[39] T. C. Chuang, C. F. Pai, and S. Y. Huang, "Cr-induced Perpendicular Magnetic Anisotropy and Field-Free Spin-Orbit-Torque Switching," Phys. Rev. Appl. 11, 061005 (2019).
[40] P. Wadley, B. Howells, J. Železný, C. Andrews, V. Hills, R. P. Campion, V. Novák, K. Olejník, F. Maccherozzi, S. S. Dhesi, S. Y. Martin, T. Wagner, J. Wunderlich, F. Freimuth, Y. Mokrousov, J. Kuneš, J. S. Chauhan, M. J. Grzybowski, A. W. Rushforth, K. W. Edmonds, B. L. Gallagher, and T. Jungwirth, "Electrical switching of an antiferromagnet," Science 351, 587 (2016).
[41] S. Y. Bodnar, L. Šmejkal, I. Turek, T. Jungwirth, O. Gomonay, J. Sinova, A. A. Sapozhnik, H. J. Elmers, M. Kläui, and M. Jourdan, "Writing and reading antiferromagnetic Mn2Au by Néel spin-orbit torques and large anisotropic magnetoresistance," Nat. Commun. 9, 348 (2018).
[42] X. Z. Chen, R. Zarzuela, J. Zhang, C. Song, X. F. Zhou, G. Y. Shi, F. Li, H. A. Zhou, W. J. Jiang, F. Pan, and Y. Tserkovnyak, "Antidamping-Torque-Induced Switching in Biaxial Antiferromagnetic Insulators," Phys. Rev. Lett. 120, 207204 (2018).
[43] L. Baldrati, C. Schmitt, O. Gomonay, R. Lebrun, R. Ramos, E. Saitoh, J. Sinova, and M. Kläui, "Efficient Spin Torques in Antiferromagnetic CoO=Pt Quantified by Comparing Field- and Current-Induced Switching," Phys. Rev. Lett. 125, 077201 (2020).
[44] P. Zhang, J. Finley, T. Safi, and L. Liu, "Quantitative Study on Current-Induced Effect in an Antiferromagnet Insulator/Pt Bilayer Film," Phys. Rev. Lett. 123, 247206 (2019).
[45] Y. Cheng, S. Yu, M. Zhu, J. Hwang, and F. Yang, "Electrical Switching of Tristate Antiferromagnetic Néel Order in α-Fe2O3 Epitaxial Films," Phys. Rev. Lett. 124, 027202 (2020).
[46] C. C. Chiang, S. Y. Huang, D. Qu, P. H. Wu, and C. L. Chien, "Absence of Evidence of Electrical Switching of the Antiferromagnetic Néel Vector," Phys. Rev. Lett. 123, 227203 (2019).
[47] A. Churikova, D. Bono, B. Neltner, A. Wittmann, L. Scipioni, A. Shepard, T. Newhouse-Illige, J. Greer, and G. S. D. Beach, "Non-magnetic origin of spin Hall magnetoresistance-like signals in Pt films and epitaxial NiO/Pt bilayers," Appl. Phys. Lett. 116, 022410 (2020).
[48] T. Matalla-Wagner, Jan-Michael Schmalhorst, Günter Reiss, Nobumichi Tamura, and Markus Meinert, "Resistive contribution in electrical-switching experiments with antiferromagnets," Phys. Rev. Res. 2, 033077 (2020).
[49] D. Hou, Z. Qiu, E. Saitoh, "Spin transport in antiferromagnetic insulators: progress and challenges," NPG Asia Mater. 11, 35 (2019).
[50] Yi-Hui Zhang, Ting-Wei Weng, Tsao-Chi Chuang, Danru Qu, and Ssu-Yen Huang, "Demonstration of Spin Current Switch across Ferro-Antiferromagnetic Transition," Adv. Quantum Technol., 3 20200059 (2020).
[51] V. P. Amin and M. D. Stiles, "Spin transport at interfaces with spin-orbit coupling: Formalism," Phys. Rev. B 94, 104419 (2016).
[52] C. O. Pauyac, M. Chshiev, A. Manchon, and S. A. Nikolaev, "Spin Hall and Spin Swapping Torques in Diffusive Ferromagnets," Phys. Rev. Lett. 120, 176802 (2018).
[53] A. M. Humphries, T. Wang, E. R. J. Edwards, S. R. Allen, J. M. Shaw, H. T. Nembach, J. Q. Xiao, T. J. Silva, and X. Fan, "Observation of spin-orbit effects with spin rotation symmetry," Nat. Commun. 8, 911 (2017).
[54] M. Kimata, H. Chen, K. Kondou, S. Sugimoto, P. K. Muduli, M. Ikhlas, Y. Omori, T. Tomita, A. H. MacDonald, S. Nakatsuji, and Y. Otani, "Magnetic and magnetic inverse spin Hall effects in a non-collinear antiferromagnet," Nature 565, 627 (2019).
[55] T. Wang, S. Lendinez, M. B. Jungfleisch, J. Kolodzey, J. Q. Xiao, and X. Fan, "Detection of spin-orbit torque with spin rotation symmetry," Appl. Phys. Lett. 116, 012404 (2020).
[56] T. C. Chuang, D. Qu, S. Y. Huang, and S. F. Lee, "Magnetization-dependent spin Hall effect in a perpendicular magnetized film," Phys. Rev. Res. 2, 032053 (2020).

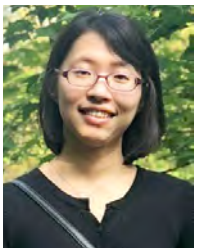

Danru Qu is currently a postdoctoral Fellow at Academia Sinica, Taiwan. She was a JSPS postdoctoral fellow in the Institute for Solid State Physics at the University of Tokyo. She obtained her PhD from the Johns Hopkins University and received her BSc degree from the University of Science and Technology of China. Her current research focuses on spintronics, spin caloritonics, magnetic Weyl semimetals, and quantum materials.

Ssu-Yen Huang is an associate professor in the Department of Physics at National Taiwan University. After receiving his Ph. D. in Electrophysics from National Chiao Tung University, he worked as a postdoctoral research fellow subsequently at Academia Sinica, National Tsing Hua University, Massachusetts Institute of Technology, and Johns Hopkins University. He is an experimentalist in condensed matter physics and his current research focuses on spintronics, spin caloritonics, and pure spin current phenomena.